IOP Conf. Series: Materials Science and Engineering **758** (2020) 012013 doi:10.1088/1757-899X/758/1/012013

Analysis of Insulation Structure Design for High Altitude UHV Reactor Bushing

Zhang Shiling

1 State Grid Chongqing Electric Power Company Chongqing Electric Power Research Institute, Chongqing, 401123
E-mail: 526793305@qq.com

Abstract. The ultra high voltage reactor bushing is the important equipment to realize the electrical connection between the reactor and the valve tower. The high altitude application environment puts forward higher requirement for electrical structure design of reactor bushing. The paper mainly discusses the design of the internal and external insulation structure. The design and analysis of the tail of the bushing, the corona ring and the inner insulation of bushing have been done. The three dimensional electric field simulation model has been set up to calculate and analyze the insulation performance of the bushing. The results show that the elevation correction of the external ring and the flash-over voltage of the porcelain under high altitude should be done, and the calculation shows that the correction coefficient are 2.07 and 1.36 respectively, and the end of bushing should install with double type ring. The insulation distance of the hollow composite insulator is designed as 8500mm. The insulation distance of the bushing tail is designed as 1955mm. The maximum field strength of the corona ring is 1.251kV·mm^{-1}, and maximum field strength on the surface of tail corona ring is 16.96kV·mm^{-1}. The axial field strength of the bushing core near center conductor is higher than the flange side, and the maximum field strength is 0.55kV·mm^{-1}. The results of the paper can provide the theoretical basis for the design of the insulation of the reactor transformer bushing used in the UHV transmission project.

1. Introduction

The structure of the high-voltage capacitive bushing is complex, involving many insulating media and withstanding high voltage in narrow and long insulating space. Therefore, it is difficult to design the internal and external insulation structure of high-voltage capacitive bushing. For reactor bushing, the structure of the outer ceramic sleeve with the oil-immersed paper capacitor core is generally adopted at present. The insulation coordination between outer insulation of ceramic sleeve and inner insulation of core is the key link in the design[1,2]. On the other hand, the research object of this paper is high altitude and UHV reactor bushing. High altitude and UHV indicate that the operation environment of this bushing is special[3,4]. In high altitude condition, the structural parameters of outer insulation of bushing need to be revised to ensure that no flash-over accident occurs. In UHV condition, the inner insulation of bushing needs to be designed compactly to ensure that no partial discharge and internal breakdown occurs in the inner insulation of core under UHV application environment.

In view of this, the electrical structure parameters of UHV reactor bushing are firstly analyzed, and the elevation correction factor K is introduced to modify the ceramic bushing structure of reactor bushing. At the same time, the top equalizing cover structure of reactor bushing is designed according to Peek formula. Considering that the overall immersion of bushing tail structure in transformer oil is less affected by elevation, and its electrical structure parameters are designed according to the traditional

calculation method[5-7]. Based on the reasonable design of the inner and outer insulation structure of the reactor bushing, the internal insulation structure is optimized by using the equal margin method, and the reactor bushing pressure equalizing ring with reasonable structure is configured. The three-dimensional electric field simulation model of high altitude reactor bushing is established, and the electric field distribution at the key position of bushing is checked and calculated. The insulating performance of outer ceramic sleeve of high altitude reactor bushing under lightning impulse voltage is discussed, and the corona condition of the voltage equalizing cover and ceramic sleeve at the end of bushing under actual operation conditions is also discussed.

This paper focuses on the design method of internal and external insulation structure of the reactor bushing under high altitude and UHV conditions, discusses the design scheme of altitude correction coefficient and internal insulation margin under UHV conditions, and uses three-dimensional finite element method to check and calculate. The research results and data in this paper can provide reference for the design of internal and external insulation structure of reactor bushing under high altitude and UHV conditions, and also provide theoretical and practical basis for the operation and maintenance of oil-immersed paper bushing.

2. Electrical structure parameters of UHV reactor bushing

2.1. Design of dry arc distance for outer porcelain sheath of reactor bushing

The outer insulation level of reactor bushing in the high altitude substation is 960kV, the peak value of lightning impulse test voltage is 2100kV, the peak value of operating impulse test voltage is 1550kV, and the main arc distance of bushing is more than 7400mm. The structural parameters of the outer contour of the UHV reactor bushing are shown in Fig. 1.

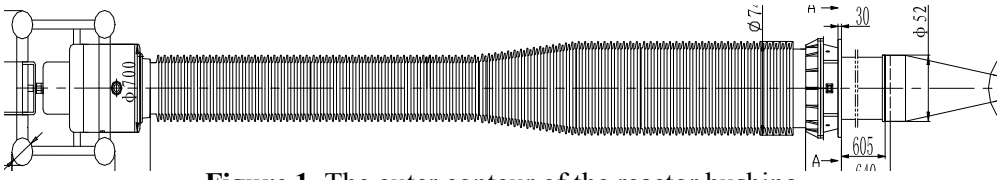

Figure.1 The outer contour of the reactor bushing

According to the requirements of GB/T4109 "insulating bushing with AC voltage higher than 1000V", altitude correction should be carried out for the external insulation level above 1000m. The altitude correction factor K is calculated according to equation (1)[8-10]:

$$K = e^{q\frac{(H-1000)}{8150}} \qquad (1)$$

For the lightning impulse voltage, withstand voltage coefficient q=1, the short-term power frequency withstand voltage q = 1 for air gap and bushing hollow composite insulator. The elevation of high-altitude substation is H = 3500m, and K = 1.36 is calculated in the entrance formula (1). The valid value of power frequency test voltage is 1305kV, the peak value of lightning impulse test voltage is 2855kV, and the peak value of operation impulse test voltage is 1950kV.

Under the power frequency and impulse voltage, the electrical performance of bushing requires that flash-over discharges can not occur on the outer surface of hollow ceramic sleeve in air or on the outer surface of the bushing core in oil. The key to the design of external insulation of the bushing is the coordination of the internal and external insulation of bushing and the regulation of main insulation of core. The dry flash-over voltage of hollow composite insulator is close to the air gap breakdown voltage between the upper flange and the middle flange, which mainly depends on the dry flash-over distance L_d. The relationship between the flash-over voltage and the dry flash-over distance is shown in Fig.2. The above figure shows that the flash-over voltage of the bushing hollow composite insulator increases with the increase of insulation distance, and there is the saturation effect. Existing formula (2) quantitatively fits the curve of Figure 2[11-13], and the fitting results are shown in Table 1.

$$U_{f50} = AL_{\mathrm{d}}^{B} \qquad (2)$$

In the formula: U_{f50} is the flash-over voltage value (discharge probability 50%)/kV; L_d is insulator dry flash-over distance/m; A and B are undetermined coefficients.

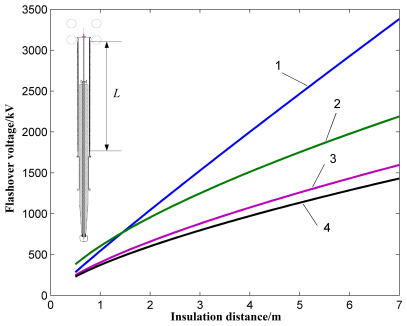

Figure.2 The relationship between flash-over voltage and insulation distance of hollow composite insulator

Table.1 Quantitative relationship between flash-over voltage and insulation distance of composite insulator

Test Voltage Type	*A*	*B*
Lightning Full Wave Shock Dry/Wet Flash Voltage	545.5	0.9377
Positive Operating Dry/Wet Flash Voltage	603.4	0.6624
Power Frequency Dry Flash-over Voltage (RMS)	404.6	0.7053
Power Frequency Wet Flash-over Voltage (RMS)	372.3	0.6921

Combined formula (1) and formula (2) are used to calculate the dry arc distance of outer insulation of bushing and porcelain sleeve (3):

$$L_d = (Te^{q\frac{H-1000}{8150}})^{\frac{1}{B}} \qquad (3)$$

Coefficient among them $T = (MU_{design})/A$, M is the insulation design margin, U_{design} is the voltage value under the different voltage types. Formula (3) shows that the altitude, test voltage and insulation design margin are positively correlated with the distance of the bushing dry arc. Setting the insulation margin as M=1.2, combined with the test data in Table 1 and (3) formula, the dry arc distance of the outer insulation of UHV reactor bushing under lightning impulse test voltage 2100kV is 7093 mm. Similarly, the dry arc distance of the outer insulation of bushing porcelain bushing under the power frequency wet flash-over voltage 960kV and the positive operation wave dry/wet flash-over voltage 1550kV can be calculated. The arc distances are 7967 mm and 8494 mm, respectively. Considering the manufacturing specifications, the dry flash-over distances of the ceramic sleeve of the reactor sleeve are designed to be 8500 mm. The outline of the ceramic sleeve is shown in Figure 3.

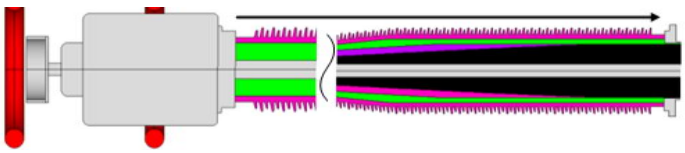

Figure.3 The outline of the outer porcelain of reactor bushing

2.2. Design of Reactor Bushing Tail Distance

Reactor bushing tail is immersed in transformer oil, so its flash-over voltage is not limited by bushing operation in the high altitude area. In insulation structure design, it can be considered according to conventional bushing size[14]. In order to ensure that no flash-over occurs at the tail of capacitor core under the RMV of power frequency test voltage 960kV (without altitude correction), the axial field strength is set to 0.6kVmm^{-1} in the main insulation design of bushing, so the total length of lower step is 960/0.6 = 1600 mm. Considering the actual winding conditions of bushing core, the insulation

distance at the tail of bushing is determined. The design is 1955 mm, and the tail design is shown in Fig. 4. The bushing tail equalizing cover is used to shield the connection area between the central guide rod and the transformer winding, and the insulation medium at the bushing tail is complex, including bushing oil, porcelain bushing, oil-immersed insulation paper, etc. [15]. The electric field distribution of the bushing tail equalizing cover needs to be further checked and calculated.

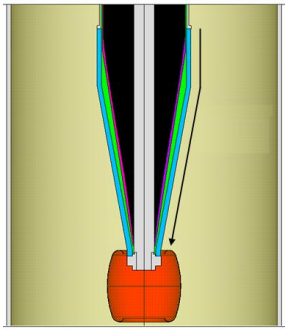

Figure.4 The condenser tail of the reactor bushing

2.3. Design of corona equalizing cover for bushing

In order to improve the flash-over voltage of the outer ceramic sleeve of the reactor bushing, it is necessary to configure the reasonable end pressure equalizing cover to uniformly distribute the voltage along the ceramic sleeve. In addition, there are some key structural components at the end of the sleeve, such as the junction plate, confluence fittings, bus lead-out line, etc. After installing pressure equalizing ring at the end of the sleeve, the sharp corners and protrusions on the surface of the above irregular conductors can be effectively shielded, and the corona discharge and the resulting external insulation flash-over can be suppressed .

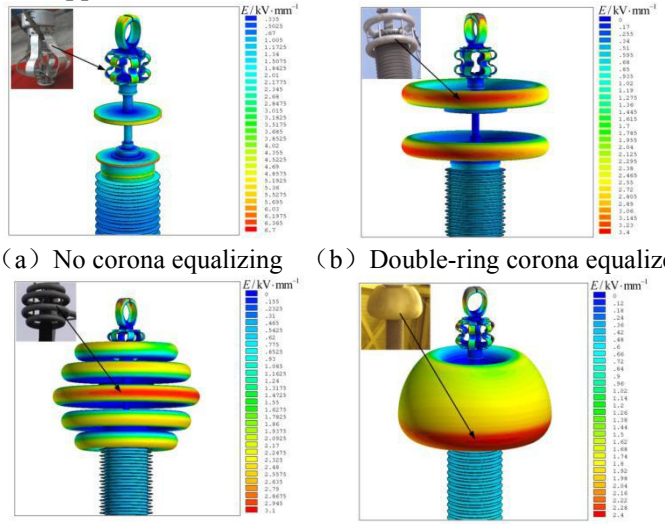

（a）No corona equalizing （b）Double-ring corona equalizer

（c）Multi-ring corona equalizer（d）Apple type corona equalizer

Figure.5 The structure of high voltage bushing corona ring

As shown in Fig. 5 (a), in absence of the pressure equalizer, the high field strength area is concentrated at the edge of the confluence metal, the maximum field strength is 6.7kV mm^{-1}, which is higher than the breakdown field strength of air 3kVmm^{-1}. Therefore, corona discharges will occur at the edge of the metal. After installing the double-ring pressure equalizer, the confluence metal is located at the low field strength inside pressure equalizer. The maximum field intensity is reduced to 3.4kVmm^{-1}, which appears on surface of the equalizing cover, as shown in Fig. 5 (b). In order to further improve the electric field distribution at the end of the bushing, the structure of multi-ring pressure equalizer can be adopted. As shown in Fig. 5 (c), it can be seen that the position where the maximum electric field intensity occurs shifts to the middle part of the pressure equalizer, and the maximum electric field intensity is 3.1kVmm^{-1}. The double-ring and the multi-ring pressure equalizing covers have practical

application in high-voltage substation. Apple-shaped pressure equalizing covers are generally used at the end of power equipment in valve hall of high-voltage converter station, as shown in Fig. 5 (d). It can be seen that the apple-type pressure equalizer can completely cover the confluence metal in the low field strength area, and the electric field distribution on the surface of the pressure equalizer is uniform. The maximum electric field strength is 2.4kVmm^{-1}, which is lower than the breakdown field strength of the air 3kVmm^{-1}. However, it is difficult to manufacture the apple-type pressure equalizer. Considering the manufacturing cost and installation difficulty, the shroud of transformer substation reactor bushing end equalizer generally adopts double-ring structure, but the structure size needs to be further enlarged.

2.4. Insulation structure design of reactor bushing

On the basis of the insulation structure design of the outer porcelain sleeve and the tail of the core of the reactor bushing, the internal insulation structure design of the reactor bushing is further developed. Because the running environment of the bushing is at high altitude, the coordination between the inner insulation structure and the outer insulation of the reactor bushing should be considered in particular. In the design, the dry arc insulation length of the outer ceramic bushing is 8500 mm, the length of the inner plate is 6645 mm, and the length of the outer plate is 1665 mm. The inner plate shields the outer ceramic bushing. The percentage of distance is (6645-1955)/8500=55.2%. It has better shielding effect in theory to lengthen the insulating distance of dry arc, but the longer zero-layer plate makes it more difficult to roll capacitor core. After detailed design and calculation, the design parameters of the insulation structure in the bushing of high-altitude reactor are shown in Table 2.

Table.2 Design parameters of insulation structure of high altitude reactor bushing

Plate sequence number	Plate length	Plate diameter	layer thickness
0	6645	115.0	/
10	6293	133.0	1.0
30	5504	180.0	1.4
50	4602	243.6	1.8
70	3625	319.2	1.9
90	2671	392.2	1.7
110	1843	446.2	1.1

Table 2 shows that the number of design layers of high altitude reactor bushing reaches more than 100 layers. This design can maximize the potential distribution on the surface of the bushing porcelain jacket by using the voltage equalization effect of capacitance structure, and raise the critical flash-over voltage of the bushing porcelain jacket. At the same time, Table 2 shows that the thickness of the inner insulation structure increases first and then decreases with the inverted "U" distribution. The actual design calculation results are consistent with the theoretical calculation, which proves to some extent the rationality of the design of the inner insulation structure of the reactor bushing.

3. Design Checking Calculation Based on Finite Element Electric Field Simulation

3.1. Establishment of calculation model for reactor bushing

According to the design dimensions of the outer ceramic sleeve dry arc distance, the tail distance of the reactor sleeve, the pressure equalizing cover of the sleeve and the internal insulation structure, the simulation calculation model of the high altitude reactor sleeve is established under the finite element simulation environment, as shown in Figure. 6.

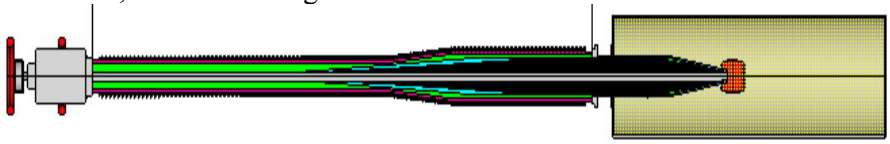

Figure.6 The FEM calculation model of the reactor bushing

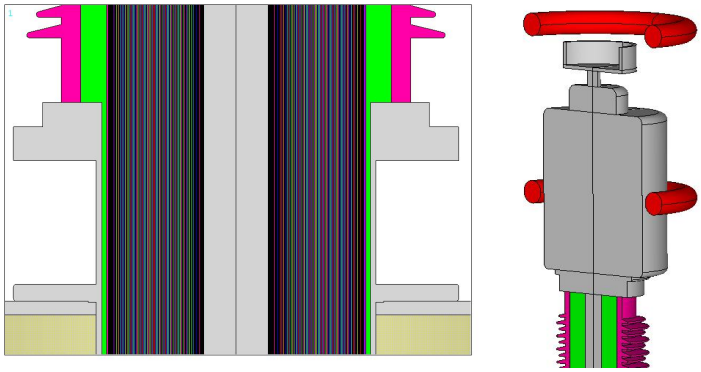

Figure.7 The FEM model of main insulation of reactor bushing

In simulation calculation model, the insulation medium of reactor bushing, the top voltage equalizing cover and the tail voltage equalizing cover of bushing are also considered, especially the modeling details of the insulating pole plate in bushing are shown in Fig. 7. The model considers more than 100 layers of plates into the checking calculation, which makes the simulation results closer to the actual operating environment of UHV reactor bushing.

3.2. Calibration of Insulation Electric Field inside and outside Reactor Bushing

Lightning impulse test voltage is applied to high-potential conductor of high-altitude reactor bushing to calculate its overall potential distribution. The distribution of the overall equipotential line of the porcelain bushing outside the bushing and the distribution of the equipotential line at the tail of the bushing are shown in Figure 8. It shows that the equipotential line distribution is more uniform, and the inner pole plate of the main insulation of the bushing has better modulation effect. The equipotential line is evenly dispersed from the edge of the pole plate to gather at the top and tail of the bushing equalizing cover, and the equipotential line in the inner pole plate of the bushing is forced to be parallel to the axis of the bushing core, which ensures that the electric field distribution in the bushing core is basically uniform.

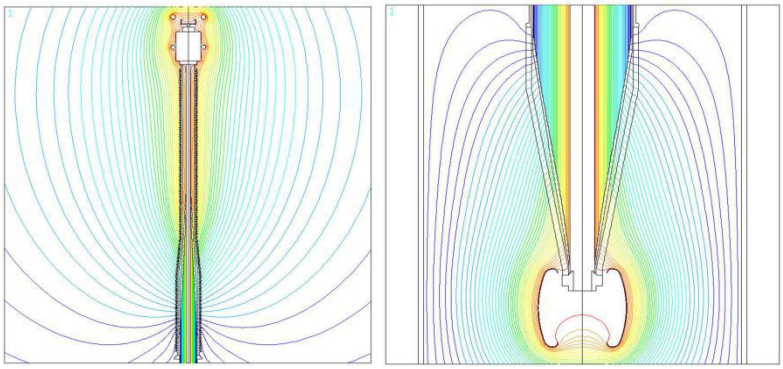

Figure.8 The distribution of equipotential line of porcelain and bushing tail

Focus on the distribution of electric field in the top and tail of reactor bushing to ensure that no visible corona occurs on the surface of the shroud. The results of E-field verification are shown in Figure 9.

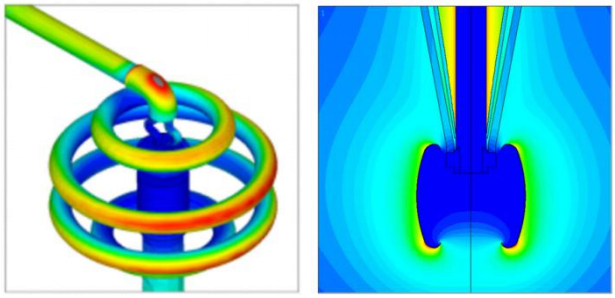

(a) Top equalizing ring (b) Tail equalizer

Figure.9 The E-field distribution of the busing corona ring

A large number of experiments conducted by Peek show that the initial field strength of corona is related to tool size, atmospheric state and surface state. Summarizing the experimental results, the corona initial field strength (peak value) can be obtained as follows:

$$E_c = 30.3m\delta(1+\frac{0.298}{\sqrt{\delta r}}) \qquad (4)$$

According to formula (4), it can be seen that the atmospheric state has a great influence on the initial field strength of corona. The reactor bushing runs at an altitude of about 3500M. When Peek formula is used, the design margin can be taken as 0.72, the altitude factor can be taken as 0.7416, the radius of equalizing ring R is 10cm, and the corona onset field strength E_c is about 1.81 kVmm^{-1}. According to the calculation and statistics, the maximum electric field intensity on the surface of the equalizing ring, which can be controlled by 0.8, can be calculated to be 1.45 kVmm^{-1} at the peak value. The corona phenomenon can hardly be seen on the top of the equalizing ring at 3500m altitude. Figure 9 shows that the electric field distribution on the surface of the reactor bushing pressure equalizing cover is uniform. The maximum electric field intensity on the surface of the top pressure equalizing ring is 1.251 kVmm^{-1} and the maximum electric field intensity on the surface of the tail pressure equalizing ring is 16.962 kVmm^{-1}, which are lower than the control electric field intensity on the surface of the metal fittings in the air and the transformer oil, respectively.

3.3. Calibration of Insulation Electric Field in Reactor Bushing

The distribution curves of potential and electric field are intercepted along the surface of the ceramic sleeve of the reactor bushing and the surface of the ceramic sleeve in the oil at the tail of the bushing respectively, as shown in Figure. 10 and 11.

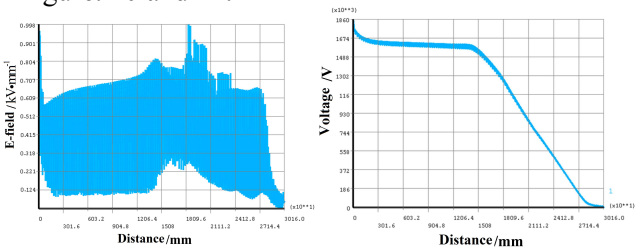

（a）E-field distribution （b）Voltage distribution

Figure.10 The E-field distribution of the bushing porcelain

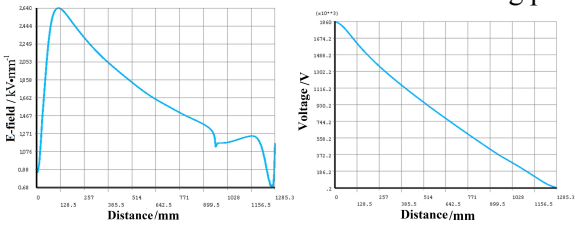

（a）E-field distribution （b）Voltage distribution

Figure.11 The E-field distribution of the bushing tail

The figure shows that the potential distribution on the outer and tail of the reactor bushing presents the linear distribution characteristics due to modulation of inner plate, while the electric field distribution increases gradually and then decreases. However, the electric field distribution on the surface of the ceramic bushing has large jump, which is mainly caused by the umbrella ridge structure on the surface of the ceramic bushing. On the other hand, the radial field intensity distribution in the capacitor core is shown in Figure 12.

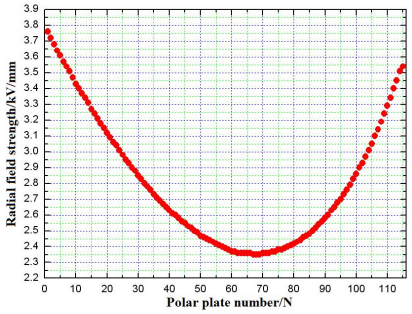

Figure.12 The radial field distribution of bushing condenser

Figure 12 shows that radial field intensity of reactor bushing core presents the typical "U" distribution characteristics of high end and low middle, and the field intensity at the interface between core and bushing core is higher. Therefore, the insulation strength at the interface between core and core conductor should be strengthened. At the same time, the distribution of field intensity at the edge of plate and the distribution of partial discharge margin between plates should be strengthened. The situation is shown in Figure 13.

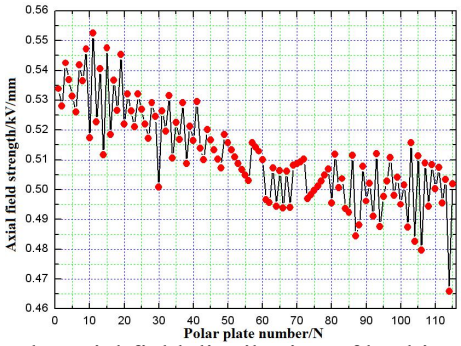

Figure.13 The axial field distribution of bushing condenser

Figure 13 shows that the axial field strength of the reactor bushing core basically presents uniform distribution, and the axial field strength near the central guide rod side is slightly higher than that at flange side, and the maximum field strength is 0.55kVmm^{-1}, which is lower than the field strength control value. And the partial discharge margin between the plates is basically uniform distribution, and its value is stable around 2.0, which has the high safety margin. The maximum field strength at the key position of the reactor bushing at high altitude under various operating conditions is summarized in Table 3. The field strength at the key position under other voltage levels can be converted according to the above data.

Tab.3 The maximum field strength at each key position of the reactor bushing/V/mm

Equalizing ring in air	Ball in oil	Porcelain Covers in Air	Surface of Porcelain Sheath in Oil	Maximum radial field strength	Maximum Axial Field Strength
1.251	16.962	0.998	2.64	3.75	0.55

4. Conclusion

1) Under the condition of high altitude, the flash-over voltage of metal fittings and porcelain jackets outside the reactor bushing should be corrected at altitude. The calculation shows that the correction coefficients of metal fittings and flash-over voltage are 2.07 and 1.36, respectively.

2) Through checking calculation, it is determined that the dry arc distance of outer porcelain sleeve of high-altitude reactor is 8500mm, the insulation distance of casing tail is 1955mm, and the double-ring pressure equalizing cover is adopted for the pressure equalizing cover.

3) Finite element calculation shows that the maximum field strength of the top equalizing ring surface is 1.251kVmm^{-1}, the maximum field strength of the tail equalizing ring surface is 16.962kVmm^{-1}, which is lower than the control field strength of the metal surface in air and transformer oil; the axial field strength near the central guide rod side is slightly higher than that on the flange side, and the

maximum field strength is 0.55kVmm^{-1}, which is lower than that in the air and transformer oil. The high-altitude reactor bushing successfully passed the lightning impulse test of 2855kV, and the corona phenomenon could not be seen at the end of the high-altitude reactor bushing under actual operation conditions, which proved that the structure design of the reactor bushing was reasonable and the electrical performance was stable under the high-altitude conditions.

Reference

[1] Zhang Xuecheng, Tan Jinhua, Niu Wanyu. Bushings design of converter transformer's valve side of UHVDC transmission project [J]. High Voltage Engineering, 2012, 38(2): 393-399.
[2] Chen Zhong, Wu Heng, Huang Heyan, et al. Cause analysis and improvement measure of ± 800kV DC wall bushing occurring flashover during overvoltage withstand test[J]. High Voltage Engineering, 2011, 37(9): 2133-2139.
[3] Toshiaki rokunohe, Tatsuro kato, Makoto hirose, et al. Development of insulation technology in compact SF6 gas-filled bushings: development of compact 800kV SF6 gas-filled bushings [J]. Electrical Engineering in Japan, 2010, 171(1): 19-27.
[4] Hosokawa M, Okumura K, Yamagiwa T, et al. Dielectric performance of improved gas insulated bushing for UHV GIS[J]. IEEE Transaction on Power Delivery, 1987, 2(2): 359-366.
[5] Dexin Nie, Hailong Zhang, Zhong Chen, et al． Optimization Design of Grading Ring and Electrical Field Analysis of 800kV UHVDC Wall Bushing[J]. IEEE Transaction on Dielectrics and Electrical Insulation, 2013, 20(4): 1361-1368.
[6] Wei Xiaoguang, Zong Wenzhi, Wang Gaoyong, et al. Experimental studies on switching impulse flashover characteristics of external insulation and altitude correction methods for±1100kV UHVDC converter valves[J]. Proceedings of the CSEE, 2014，34(12)：1996-2003.
[7] Wang Yongqiang, Ouyang Baolong, Lian Shasha, et al. Study on electric field distribution along the surface of snowed composite insulator in high altitude area[J]. High Voltage Apparatus, 2016，52(6)：115-123.
[8] Wang Jianyi, Li Jinzhong, Li Jun et al. Modification of condition assessment for HVDC equipment used in high altitude area[J]. Proceedings of the CSEE, 2016，36(17)：4786-4792.
[9] Xiao Gan, Chang Minghui, Wu Xueen et al. Analysis of insulation length change of bushing used in high altitude area[J]. Transformer, 2017，54(10)：10-13.
[10] Luo Xiaoqing, Hu Wei, Xu Zuoming, et al. Air gap flashover characteristics and selection of gap distances for ±1100kV DC U-shaped wall bushing[J].High Voltage Engineering, 2017，43(3)：946-952.
[11] Xu Jianyuan, Ren Chunwei, Si Binge, Lin Xin. Three dimensional electric field analysis of 40.5kV SF6 cubicle gas-insulated metal-enclosed switchgear [J]. Proceedings of the CSEE, 2008, 28(15): 136-140.
[12] Zhang Shiling, Peng Zongren, Wu Hao. Analysis on power loss of valve-side RIP bushing for ± 800kV converter transformer [J]. Power System Technology, 2014, 38(7): 1758-1764.
[13] Lin Xin, Li Xintao, Xu Jianyuan, et al . Research on numerical computation of SF6 breakdown voltages and spectral experiment in uniform electric fields[J]. Proceedings of the CSEE, 2016，36(1)：301-309.
[14] Wen Miao, Lin Xin, Zhong Simeng. Numerical simulation and experimental study of heat transfer characteristics in transformer bushing [J].High Voltage Engineering, 2016， 42(9)： 2956-2961.
[15] Zhang Jia, Lin Xin, Su An, et al. Experiment on breakdown characteristics of SF6/CF4 gas mixture under two typical electrode arrangements[J].High Voltage Apparatus, 2016，52(12)：93-98.